Electronic Supplementary Information

A highly stretchable and ultra-sensitive strain sensing fiber based on a porous core-network sheath configuration for wearable human motion detection

Jun Liu,‡[a] Peng Wang, ‡[a] Guoxian Li, [a] Li Yang, [b] Wei Yu,*[a] Chuizhou Meng*[a] and Shijie Guo [a]

[a] State Key Laboratory for Reliability and Intelligence of Electrical Equipment, Hebei Key Laboratory of Smart Sensing and Human-Robot Interaction, School of Mechanical Engineering, Hebei University of Technology, Tianjin, 300401, China.

[b] State Key Laboratory of Reliability and Intelligence of Electrical Equipment, School of Health Sciences and Biomedical Engineering, Hebei University of Technology, Tianjin 300130, China.

Correspondence: 2021085@hebut.edu.cn, 2018108@hebut.edu.cn

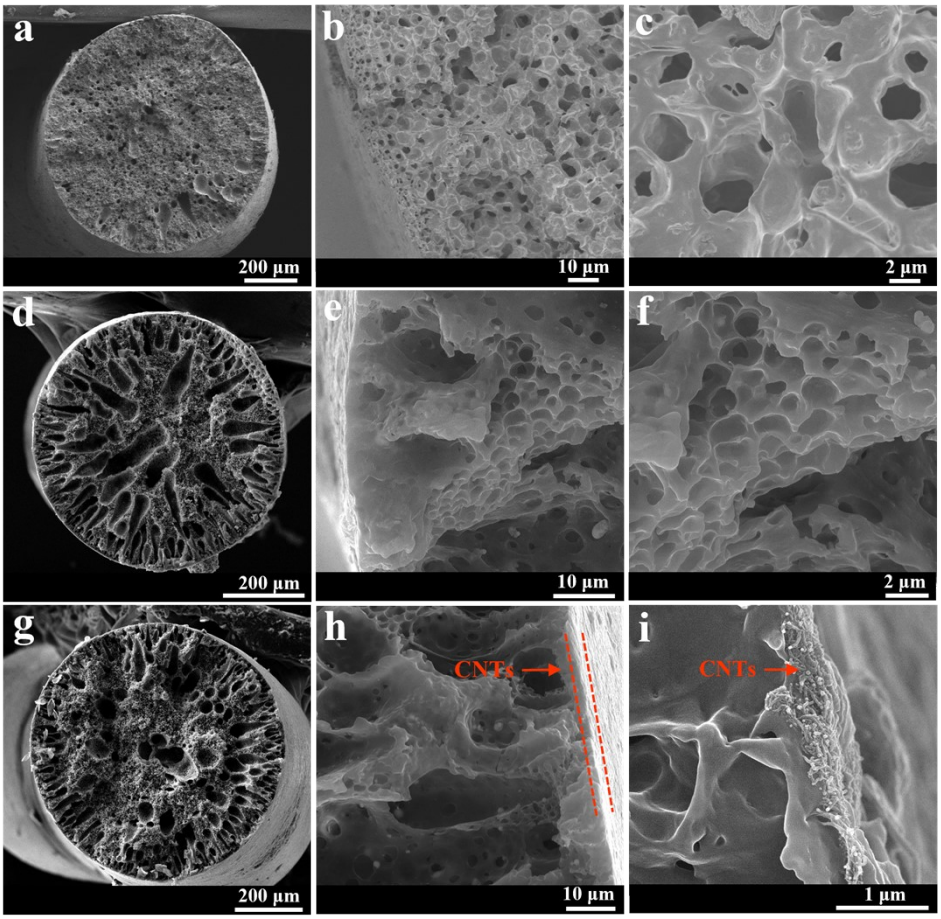

Fig. S1 SEM images of the cross section of fibers. (a) Cross section of the pristine TPU fiber. (b-c) Zoom-in views at different magnifications showing the relatively tiny pore strucutre of the pristine TPU fiber. (d) Cross section of the EGaIn/TPU fiber. (e-f) Zoom-in views at different magnifications showing the large macropore strucutre of the EGaIn/TPU fiber. (g) Cross section of CNT/EGaIn/TPU fiber. (h-i) Zoom-in views at different magnifications showing the interface between the inside prous EgaIn/TPU core and the outside CNT network theath.

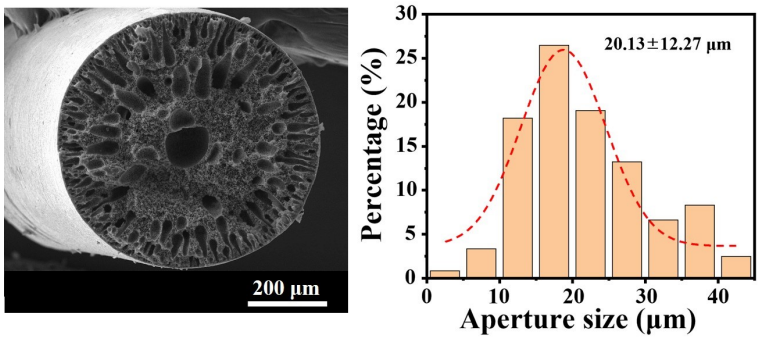

Fig. S2 Aperture statistics of pore sizes in the cross-section of fiber.

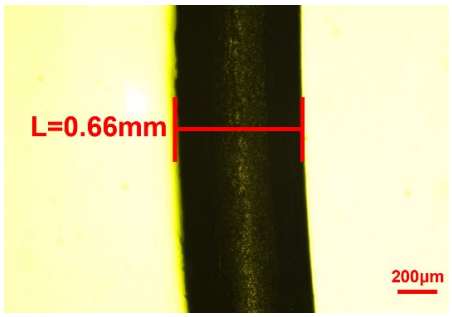

Fig. S3 Optical microscopy image of the AgNW/CNT/EGaIn/TPU fiber. The red line marks the diameter of the fiber to be about 0.66 mm.

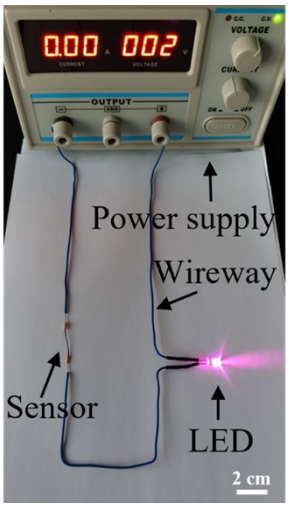

Fig. S4 Experimental setup of using the AgNW/CNT/EGaIn/TPU fiber as a flexible conductive wire to connect a LED-powering circuit. Due to the excellent electric conductivity, the LED was brightly light up by the DC power supply.

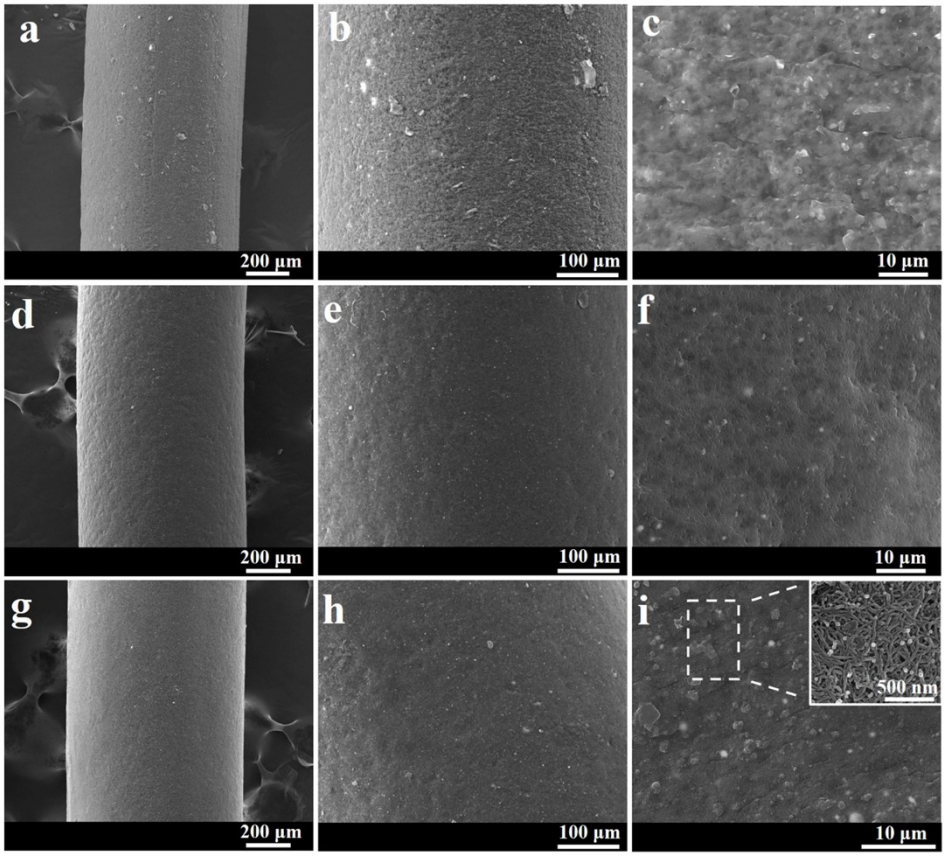

Fig. S5 SEM images of the uniform and smooth surface of fibers. (a) Surface of the pistine TPU fiber. (b-c) Zoom-in views of the pristine TPU fiber at different magnifications. (d) Surface of the EGaIn/TPU fiber. (e-f) Zoom-in views of the pristine EGaIn/TPU fiber at different magnifications. (g) Surface of the CNT/EGaIn/TPU fiber. (h-i) Zoom-in views of the CNT/EGaIn/TPU fiber at different magnifications. Inset of (i) shows the morphology of the interwined CNT network.

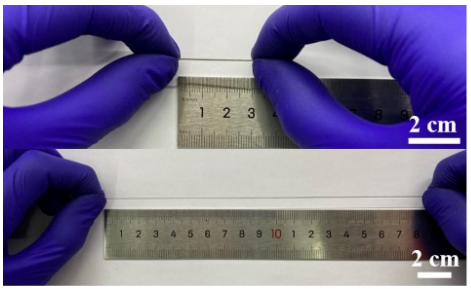

Fig. S6 Digital photos showing the AgNW/CNT/EGaIn/TPU fiber elongated at a large strain of up to 500%, indicating it has excellent tensile properties.

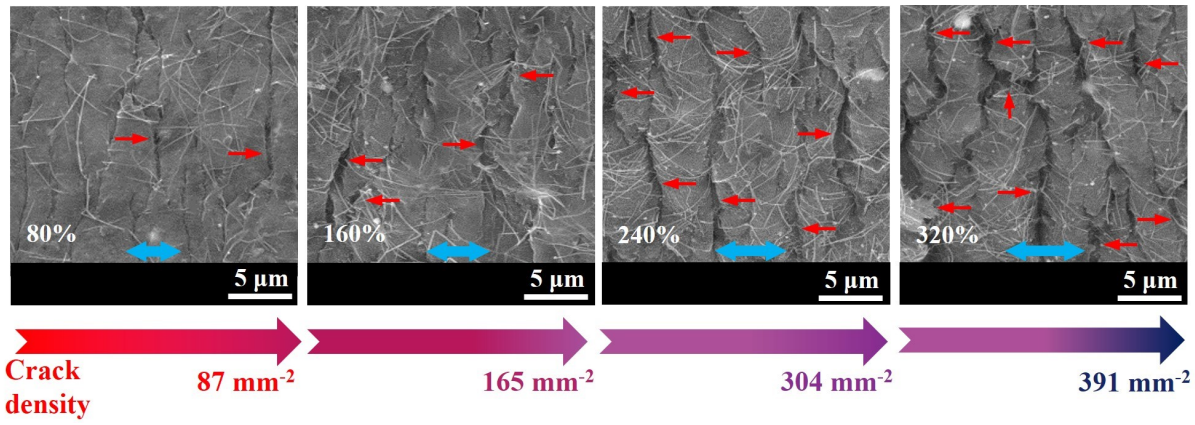

Fig. S7 SEM images of the AgNW/CNT network under different stretching strains for calculation of the crack density.

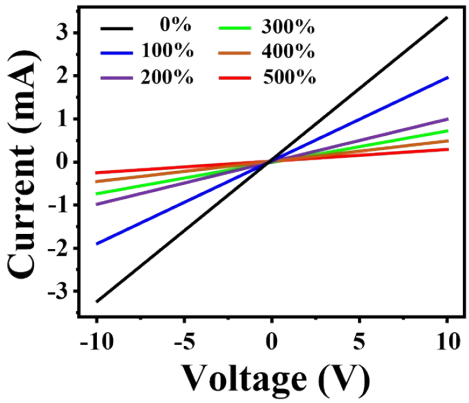

Fig. S8 I-V curves of the strain sensor under different strains.

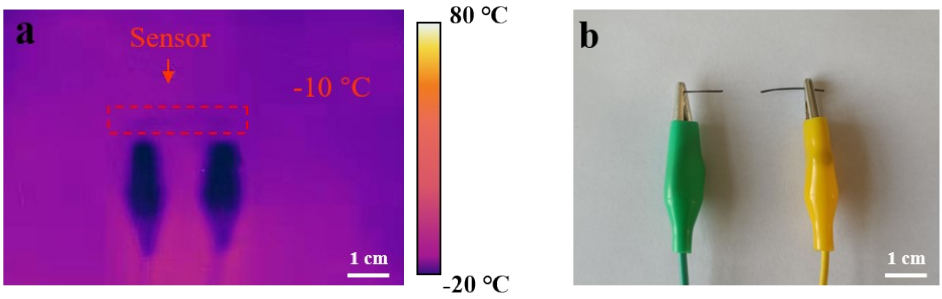

Fig. S9 Test of the AgNW/CNT/EGaIn/TPU fiber under low temperature. (a) IR image of the tensile test at -10 °C. (b) The fiber was prone to break at -10 °C.

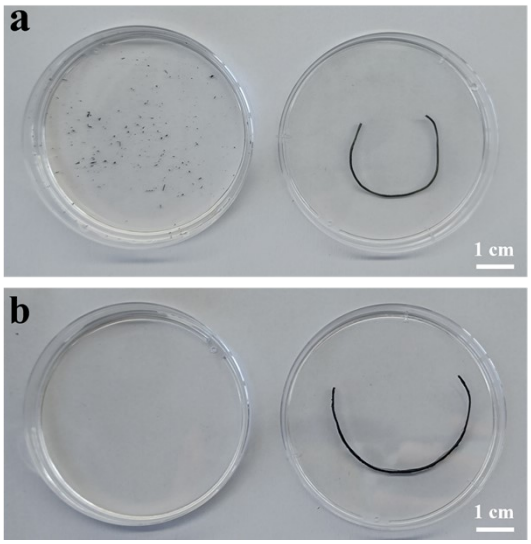

Fig. S10 Test of the AgNW/CNT/EGaIn/TPU fiber (a) without and (b) with Ecoflex encapsulation in solution. Without Ecoflex, the hydropholic AgNWs and CNTs tended to peel off from the fiber when immersed in solution especially when the fiber was repeatedly stretched and released. In comparison, with the hydrophobic Ecoflex as a protecting layer, the fiber showed no appearance detorioration at all when immersed in solution even when the fiber was heavily stretched and relesed.

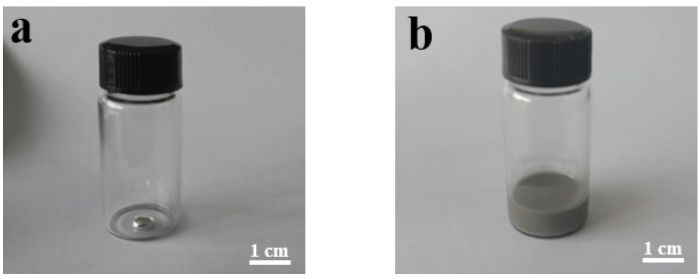

Fig. S11 Digital photo of (a) the liquid metal and (b) its solution mixture in ethanol.

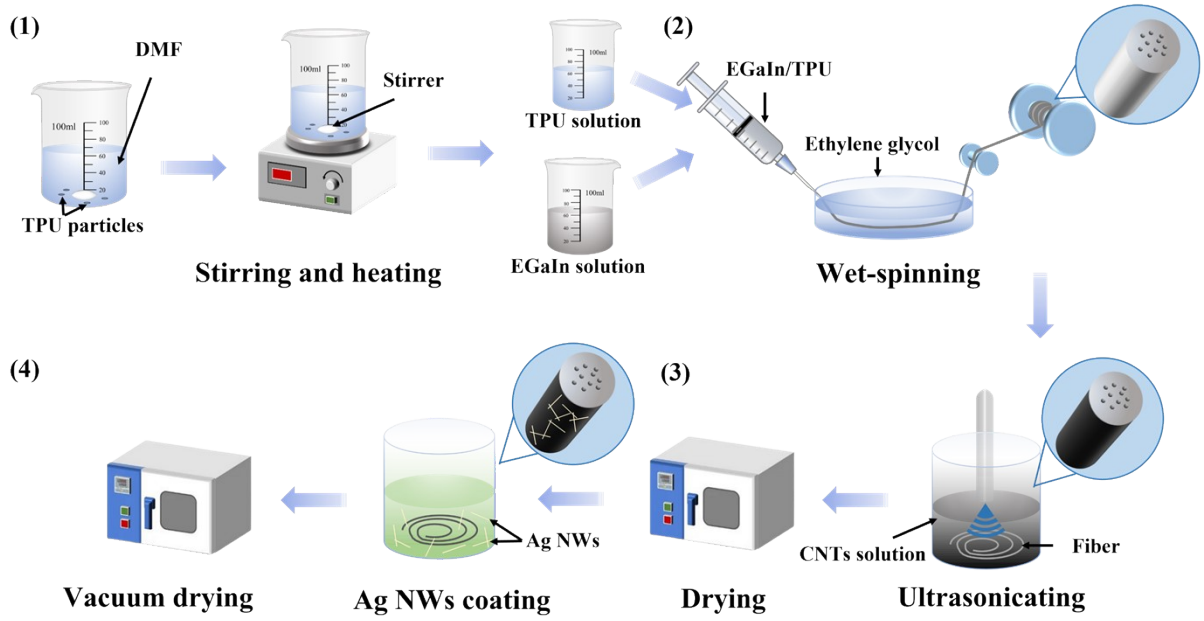

Fig. S12 Detailed fabrication process of the fiber-shaped sensor: (1) TPU solution (0.25 g mL^{-1}) was prepared by dissolving TPU pellets in DMF solvent under magnetic stirring at 65 °C for 4 h. Then the TPU solution and EGaIn solution (90 mg mL^{-1}) were evenly mixed at a ratio of 10:1 to obtain the injection solution. (2) The injection solution was steadily extruded by a 5 mL medical syringe into a coagulation bath of ethylene glycol at a rate of 0.12 mm/s. The as-spun EGaIn -embedded TPU fiber was left in the coagulation bath for 30 min to form a stable composite structure. (3) The prepared EGaIn/TPU fiber was dipped into a CNT solution (9 mg mL^{-1}) at 0 °C for 20 min with the help of probe ultrasonication with a power of 400 W to facilitate the random binding of CNTs on the surface of the fiber. Then the CNT-wrapping EGaIn/TPU fiber was dried in an oven at 70 °C for 60 min, followed by rinsing with deionized water for 1 min to remove the loosely bond CNTs. (4) The prepared CNT/EGaIn/TPU fiber was immersed into an AgNWs solution (5 mg mL^{-1}) at room temperature for 30 min to randomly bind AgNWs on the surface of the fiber. Finally the AgNW-wrapping CNT/EGaIn/TPU fiber was dried in a vacuum oven at 70 °C for 60 min to obtain the AgNW/CNT/EGaIn/TPU fiber.

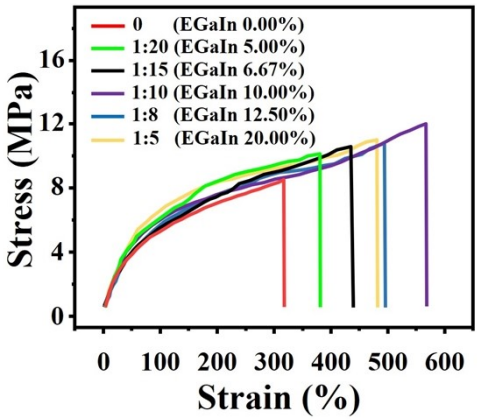

Fig. S13 Stress-strain curves of the EGaIn/TPU fibers with different volume ratios of EGaIn and TPU compared to the pristine TPU fiber.

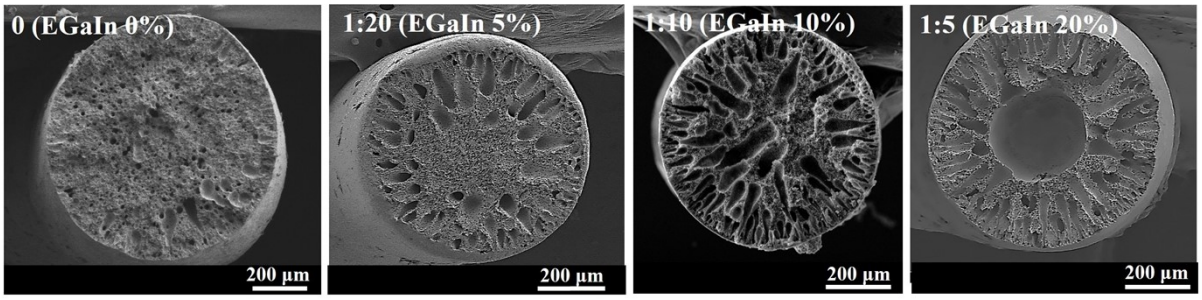

Fig. S14 SEM images of the EGaIn/TPU fibers with different volume ratios of EGaIn and TPU compared to the pristine TPU fiber.

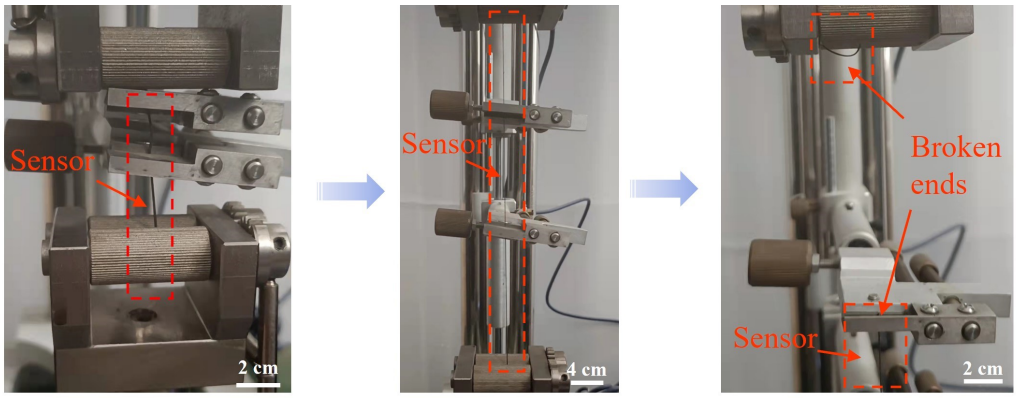

The initial state The tensile state The fracture state

Fig. S15 Digital photos showing the experimental setup of the fiber-shaped strain sensor on a tensile testing machine. The fiber was slowly and steaily stretched from its initial state until it broke into parts.

Table S1 Comparison of key performance parameters of fiber-shaped strain sensors developed in this work and reported in literature.

Configuration and Materials	Sensitivity (Max.) [GF]	Strain range (Max.) [%]	Applicability at varying temperature	Applicability underwater	Degradability and recyclability	Ref.
PU core-CNT/AgNP sheath fiber	3 249.1	150	No	No	No	1
Graphene/Yarn core-Ecoflex sheath fiber	20.7	310	No	No	No	2
Graphene/PVDF/TPU composite fiber	87	8	No	No	No	3
MWCNT core-Ecoflex sheath fiber	1 378	300	No	No	No	4
TPU core-CNT/TPU sheath fiber	166.7	350	No	No	No	5
TPU core-MWCNT sheath fiber	102	300	No	No	No	6
CNS/GNP/TPU composite fiber	144	50	No	No	No	7
SWCNT core-TPE sheath fiber	425	100	No	No	No	8
MWCNT/TPU composite fiber	97.1	320	No	No	No	9
MXene/PU composite fiber	12 900	152	No	No	No	10
Graphene/PSBS composite fiber	2 546	100	No	No	No	11
EGaIn/TPU core-AgNW/CNT sheath fiber	**7 336.1**	**500**	**Yes**	**Yes**	**Yes**	**This work**

Reference

1. B. Niu, S. Yang, X. Tian and T. Hua, *Appl. Mater. Today*, 2021, **25**, 101221.
2. W. Son, K. B. Kim, S. Lee, G. Hyeon, K. G. Hwang and W. Park, *J Nanosci Nanotechnol*, 2019, **19**, 6690-6695.
3. T. Huang, P. He, R. Wang, S. Yang, J. Sun, X. Xie and G. Ding, *Adv. Funct. Mater.*, 2019, **29**, 1903732.
4. Z. Tang, S. Jia, F. Wang, C. Bian, Y. Chen, Y. Wang and B. Li, *ACS Appl. Mater. Interfaces*, 2018, **10**, 6624-6635.
5. J. Gao, X. Wang, W. Zhai, H. Liu, G. Zheng, K. Dai, L. Mi, C. Liu and C. Shen, *ACS Appl. Mater. Interfaces*, 2018, **10**, 34592-34603.
6. Y. Yu, Y. Zhai, Z. Yun, W. Zhai, X. Wang, G. Zheng, C. Yan, K. Dai, C. Liu and C. Shen, *Adv. Electron. Mater.*, 2019, **5**, 1900538.
7. K. Ke, V. Solouki Bonab, D. Yuan and I. Manas-Zloczower, *Carbon*, 2018, **139**, 52-58.
8. J. Zhou, X. Xu, Y. Xin and G. Lubineau, *Adv. Funct. Mater.*, 2018, **28**, 1705591.
9. X. Wang, H. Sun, X. Yue, Y. Yu, G. Zheng, K. Dai, C. Liu and C. Shen, *Compos. Sci. Technol.*, 2018, **168**, 126-132.
10. S. Seyedin, S. Uzun, A. Levitt, B. Anasori, G. Dion, Y. Gogotsi and J. M. Razal, *Adv. Funct. Mater.*, 2020, **30**, 1910504.
11. X. Wang, S. Meng, M. Tebyetekerwa, Y. Li, J. Pionteck, B. Sun, Z. Qin and M. Zhu, *Composites, Part A*, 2018, **105**, 291-299.